International Journal of Applied Earth Observation and Geoinformation xxx (2012) xxx–xxx

Contents lists available at SciVerse ScienceDirect

International Journal of Applied Earth Observation and Geoinformation

journal homepage: www.elsevier.com/locate/jag

Short communication

Fractional vegetation cover estimation in arid and semi-arid environments using HJ-1 satellite hyperspectral data

Xianfeng Zhang[a,*], Chunhua Liao[a], Jonathan Li[b], Quan Sun[a]

[a] Institute of Remote Sensing and GIS, Peking University, 5 Summer Palace Road, Beijing 100871, China
[b] Department of Geography and Environmental Management, University of Waterloo, 200 University Avenue West, Waterloo, Ontario N2L 3G1, Canada

ARTICLE INFO

Article history:
Received 16 December 2010
Accepted 9 July 2012

Keywords:
HJ-1 satellite
Hyperspectral imager
Fractional vegetation cover
Atmospheric radiation correction
Dimidiate pixel model

ABSTRACT

This paper evaluates the usefulness of the hyperspectral imager (HSI) onboard Chinese HJ-1-A small satellite in vegetation mapping. Fractional vegetation cover (FVC) is an important surface microclimate parameter for characterizing land surface vegetation cover as well as the most effective indicator for assessing desertification and crop growth condition. The HJ-1/HSI data were used to calculate the narrow band vegetation index by using the in situ plot FVC data, which was then applied in sub-pixel de-composition model for the FVC estimation, namely the dimidiate pixel model. The FVC information in the Shihezi Area, Xinjiang, China was retrieved based on the dimidiate pixel model. Cross-checked with the in situ measured FVC data, a correlation coefficient square of 0.86, and the root mean square error of 10.9% is statistically achieved. The verification indicates that the FVC result retrieved from the HJ-1/HSI data is well correlated with the in situ measurements, demonstrating that the HJ-1/HSI data are promising for studying the potential impacts of global climate change on the arid and semi-arid landscapes.

1. Introduction

Vegetation is a general term for the plant community on the ground surface, such as forests, shrubs, grassland and agricultural crops, and it can intercept rainfall, alleviate runoffs, prevent desertification and conserve soil and water. It plays an important role in energy exchange, biogeochemical and hydrological cycling processes on the land surface as an "indicator" for studying global changes (Kutiel et al., 2004; Steffen, 2003). Fractional vegetation cover (FVC) refers to the percentage taken by the vertical projected area of vegetation (including leafs, stem and branches) in the total statistical area (Jing et al., 2010; Godínez-Alvarez et al., 2009; Anatoly et al., 2002; Purevdor et al., 1998; Bonham, 1989). It is an important parameter for describing the surface vegetation, a comprehensive quantitative variable for plant community on ground surface, and a basic data for characterizing ecosystems, playing an extremely crucial role in the study of regional ecosystems (Jing et al., 2010; Godínez-Alvarez et al., 2009; Steffen, 2003; Shoshany et al., 1996; Brazel and Nickling, 1987). For example, vegetation cover is one of the most common parameters used in assessing the relationship between vegetation and soil erosion. In general, soil erosion decreases with an increase in vegetation cover (Wen et al., 2010).

In terms of the state-of-art and development trend in the research on the FVC estimation, the methods roughly include ground survey, remote sensing and a combination of the two (Tammervik et al., 2003; Gutman and Lgnatov, 1998). Ground survey is a conventional method for monitoring the FVC. Early in the 1970s Muller and Ellenberg (1974) conducted a systematic research on the general method for ground survey of the FVC. Dymond et al. (1992) then measured the FVC of grassland by raster point sampling; Elvidge and Chen (1995) measured the FVC of shrubs and woodland by the photo random point method; Senseman et al. (1996) measured the FVC by the resection method; and Purevdor et al. (1998) used color digital images acquired by a digital camera to measure the FVC by counting the green pixels in the image.

With the digital camera, the FVC estimation becomes easier, faster and more accurate. Image processing software packages (e.g. Photoshop and ERDAS Imagine) can be employed to retrieve the FVC information, which is the percentage of the vegetation pixels in the total number of pixels (Zhou, 1996). White et al. (2000) used an agricultural digital camera to measure the FVC of the arid ecological system in the United States and their results showed that the agricultural digital camera is effective and accurate for long-term monitoring of the arid ecosystem (White et al., 2000). After comparing various fractional vegetation cover measuring techniques, the digital camera is considered a relatively easy and reliable ground survey technique for verifying the FVC information retrieved from remotely sensed data (White et al., 2000).

* Corresponding author. Tel.: +86 10 62759123; fax: +86 10 62759123.
E-mail address: xfzhang@pku.edu.cn (X. Zhang).

0303-2434/$ – see front matter © 2012 Elsevier B.V. All rights reserved.
http://dx.doi.org/10.1016/j.jag.2012.07.003

Although the digital camera can provide the FVC information in the plant quadrate with higher accuracy for a smaller range, it is unlikely to do so for a larger range. Remote sensing provides the possibility for large scale or even global monitoring of the FVC (Anatoly et al., 2002; Wang et al., 2002). Some methods for retrieval of the FVC using remotely sensed data have been developed, and the main ones include empirical, vegetation index, sub-pixel unmixing models (Zhou and Robson, 2001; Choudhury, 1987; Asrar et al., 1992), and linear spectral mixture models (Wu and Peng, 2010). The linear regression models were applied in many cases. For instance, in an area of semi acid soil, Graetz et al. (1988) estimated the FVC of the sparse grassland using the linear regression model based on the Landsat TM band 5 and the measured data of the FVC. Dymond et al. (1992) estimated the FVC of the degraded grassland in New Zealand utilizing the SPOT data on the basis of having built the non-linear empirical relation between the surface FVC and the normalized difference vegetation index (NDVI). Wittich and Hansing (1995) established the empirical model between the FVC and NDVI for different land cover types, and calculated the FVC using the NOAA's Advanced Very High Resolution Radiometer (AVHRR) data. Purevdor et al. (1998) built four non-linear models by applying the empirical model, to assess the FVC in Mongolia and Japan's grassland areas. In addition, by establishing a quadratic polynomial relation between the FVC and vegetation index, grassland FVC can be more accurately estimated using AVHRR data. North (2002) conducted linear regression using the ERS-2 along Track Scanning Radiometer (ATSR-2) data with four bands (555 nm, 670 nm, 870 nm and 1630 nm) in relation to the FVC and Leaf Area Index (LAI). The results showed that the linear mixed model combining four bands was more effective than the simple vegetation index in estimating the FVC. The empirical model relies on in situ measurement data in specific regions, and the measured result is fairly accurate only if the study area is small. The accuracy will be substantially reduced in large scale application and monitoring as there will be many constraints.

The basic idea of vegetation index method is that by an analysis of the vegetation types and their distribution patterns in the pixels, a conversion between vegetation index and the FVC is established for direct extraction of the FVC information, provided that the vegetation index being used is proven to be well correlated to the FVC. Using AVHRR data, Quamby et al. (1992) established a mixed linear conversion model between vegetation index and the FVC, suitable for estimating the FVC in the agricultural area. More than 40 types of vegetation indexes have currently been defined (e.g. perpendicular vegetation index (PVI), normalized differential vegetation index (NDVI), soil-adjusted vegetation index (SAVI), modified soil-adjusted vegetation index (MSAVI), transformed soil adjusted vegetation index (TSAVI), and vegetation condition index (VCI)), all have found wide application in areas like environment, ecology and agriculture (Li et al., 2010; Boles et al., 2004; Bannari et al., 1995; Leprieur et al., 1994; Dunean et al., 1993; Verstraete et al., 1993). Compared to the regression model, the vegetation index is of a greater practical significance, as it does not need ground quadrate measuring over large areas, and once verified, the model can be applied to large areas to formulate universally applicable calculation method for the FVC. However, this method may be less accurate than the empirical model in estimating the FVC in certain localities, and an accurate conversion relationship between vegetation index and the FVC is usually difficult to be determined.

The pixel decomposition method has been increasingly studied and used to derive the FVC in recent years. The pixel decomposition method can be regarded as an improvement on the basis of the vegetation index method. The idea is that a pixel in the image may actually consist of several components, each of which contributes a part of the information as observed by the remote sensor. Therefore the remote sensing information (band or vegetation spectral index) can be decomposed to build the pixel decomposition model, which is used for estimating the FVC (Gutman and Lgnatov, 1998; Tammervik et al., 2003). The dimidiate pixel model assumes that a pixel consists of only two parts: vegetation and non-vegetation, with the spectral information being just a linear synthesis of the two parts. And the ratio of the area taken by each part in the pixel will be its weight, where the percentage of the area of vegetation in the pixel will be the FVC of that pixel, and the FVC is thus estimated using this model. On the basis of the dimidiate pixel model, Gutman and Lgnatov (1998) put forward different methods for calculation of the FVC, depending on whether the pixel was homogeneous or mixed, where the mixed pixel was further divided into equal density, non-density and mixed density sub-pixels, to establish vegetation coverage models for different sub-pixel structures respectively (Jing et al., 2010; Jiang et al., 2006; Gutman and Lgnatov, 1998).

The surface biophysical parameters retrieved using remotely sensed data has become the principal means for measuring and monitoring vegetation coverage (Neigh et al., 2008; Chen, 1999; Price, 1992), although currently multispectral remote sensing data is mainly used in extraction of the FVC of large areas or on a global scale. With some new types of hyperspectral sensors orbiting the Earth, access to hyperspectral data is becoming increasingly easier. Therefore it is particularly meaningful to discuss finer and dynamic vegetation mapping for medium and small areas by using the hyperspectral data (Sykioti et al., 2011). This study attempts to discuss how the imaging spectrometer data from the HJ-1 small satellite is used in building the pixel decomposition model, for more accurately monitoring and analyzing the vegetation coverage in arid and semi-arid areas. At the same time, an assessment is conducted concerning the usability of the HJ-1/HSI data in vegetation monitoring.

The rest of this paper is structured as follows. Section 2 describes the hyperspectral imager onboard HJ-1 small satellite, in situ measurements and the data preprocessing process, and the methods used in the study. Section 3 introduces the implementation of the model for FVC retrieval and the results of the model. Section 4 presents an assessment of accuracy and discussion. Conclusions are drawn in Section 5.

2. Materials and methods

2.1. Study area and data collection

In the middle section of the northern slope of the Tianshan Mountains in China's Xinjiang Uygur Autonomous Region, the Shihezi area is situated on the south of the Junggar Basin, bordered by the Gurbantunggut Desert in the north, with the geographical coordinates being 80°58′–86°24′E, 44°01′–45°20′N (Fig. 1). With an average altitude of 500–800 m above sea level that varies greatly, declining from southeast to northwest, the area consists of mountains, plains and deserts. Its temperate continental climate features long and cold winter and short and hot summer, dry and scare rainfall, high evaporation, rapid rise and drop of temperature in spring and fall, respectively and sharp contrast between daytime and night temperatures. The annual average temperature is 7.5–8.2 °C, the annual precipitation is 180–270 mm, and the annual evaporation is 1000–1500 mm. The area is a typical arid climate environment with a full range of ecological types including snow cover, meadows and forests of the alpine ecosystem, hilly piedmont grassland, oasis agricultural system and the desert system in the center of the basin. The natural vegetation is highly dependent on rainfall, resulting in certain inter-annual fluctuation. The sparsely populated area with a dry climate is perfect for application of the remote sensing technique, and is favorable for research on interaction between human activity and the natural environment.

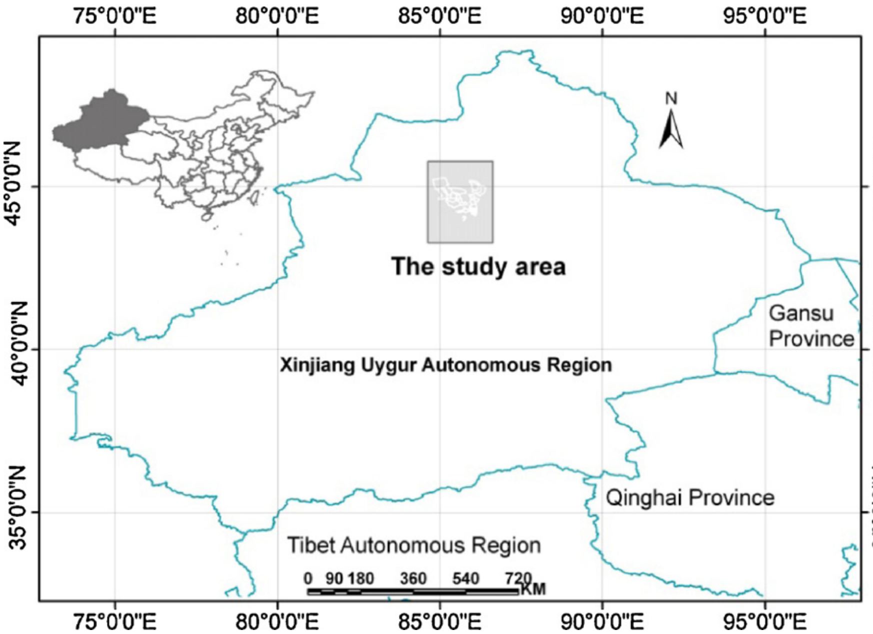

Fig. 1. Location of the study area.

HJ-1/HSI, a hyperspectral imager carried by the HJ-1-A small satellite, conducts a repeated global monitoring at a ±30° side-viewing angle, with a 96 h re-visiting cycle, a 100 m spatial resolution, a 50 km swath, 115 working bands covering a spectral range of 0.45–0.95 μm, and an average spectral resolution of 4.32 nm. Although narrow in the spectral range as compared with widely used NASA's Earth Observing System (EOS)-Moderate Resolution Imaging Spectroradiometer (EOS-MODIS) and EO-1 Hyperion, HJ-1/HSI imaging spectrometer has improved spectral resolution for better ground feature identification and information extraction. It provides another valuable tool for developing quantitative research and application such as atmospheric composition detection, water environment monitoring and vegetation growth monitoring. Table 1 summarizes the specifications of the HJ-1/HSI sensor.

The HJ-1/HSI image data covering the entire Shihezi area in Xinjiang were acquired on 24 July 2009. Three scenes of the radiometrically calibrated HSI images were used in this study. The FVC data of 65 in situ plant quadrate data in the study area were also collected (Table 2). The quadrate values falling in a same pixel were averaged to get the in situ measured value of that pixel. In the ground measuring, photograph taken by a digital camera Canon EOS500D were classified to extract the FVC by using a Decision Tree classifier. The in situ measured quadrate FVC data were mainly for assessing the accuracy of the FVC data retrieved from remotely sensed data, and for calibrating the parameters for the dimidiate pixel model.

2.2. Calibration and atmospheric radiation correction

The FLAASH module in the ENVI package was used in the atmospheric radiometric correction of the HJ-1/HSI imagery. FLAASH uses the MODTRAN4 radiometric transmission model code, and is one of the most accurate atmospheric radiometric correction models. Since no parameter is embedded in the FLAASH module for direct correction of the HJ-1/HSI data, the atmospheric radiometric correction is conducted on the basis of the HJ-1/HSI sensor's own parameters and characteristics. In the FLAASH atmospheric correction, the main parameters to be input include the central position of image, type of sensor, altitude, imaging time, mean ground elevation, image spatial resolution, the atmospheric/aerosol/water–vapor models, method for extraction of aerosol parameters, atmospheric visibility and whether spectral smoothing and wavelength re-modification are required. The HJ-1/HSI data are first to be radiometrically calibrated according to the radiometric calibration formula, then the data is converted to the BIL (band interleaved by line) or BIP (band interleaved by pixel) format. At the same time, the central wavelength of each band and its full width at half maximum (FWHM) are specified for each band. The image central position, sensor altitude,

Table 1
Specification of HJ-1/HSI sensor and data products.

Attribute	Value
Orbital altitude	649.093 km
Orbital inclination	97.9486°
Launch time	2008-9-18
Number of bands	115
Spectral range	459–956 nm
Spectral sampling	4.32 nm
Spatial resolution	100 m
Swath width	50 km
Off-nadir angle	±30 °C
Data format	HDF5
File size	82,636 (kB)
Storage format	BSQ

Table 2
Summary of the in situ plot measurements of FVC.

Plot regions (altitude range)	Plot size (m)	Number of quadrates	Land cover type
Mountainous forest (1800–2400 m)	30 * 30	5	Fir trees
Mountainous meadow (<1800 m)	1 * 1	27	High-density grassland
Mountainous mid-density grassland (<1800 m)	1 * 1	12	Mid-density grassland
Hilly areas (<1200 m)	1 * 1	10	Low-density grassland
Sporadic bush	5 * 5	3	Shrubbery
Farming land (<800 m)	2 * 2	5	Cotton and grape
Desert (<600 m)	30 * 30	3	Haloxylon ammodendron

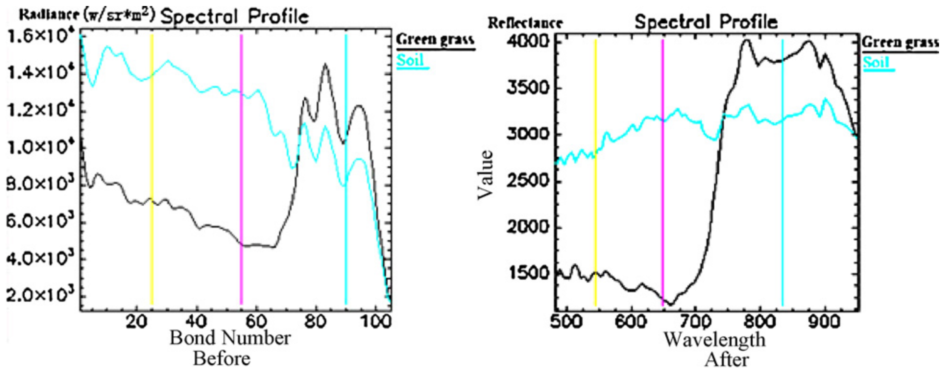

Fig. 2. The HJ-1/HSI spectra of green grass and bare soil before and after correction.

imaging time and resolution are available in the header file. The average elevation of the land surface was calculated from the digital elevation model (DEM) of the study area. The water–vapor removal model built in the FLAASH module is used to retrieve the water–vapor content in each pixel of the images. Since the HJ-1/HSI data have a spectral range from 450 nm to 950 nm, the water–vapor band should be 820 nm. When the model's parameters are correctly set up, the correction of the HJ-1/HSI data in the study area was conducted by running the FLAASH module. Fig. 2 shows a comparison of the typical surface feature spectral curve before and after the correction. On finishing the atmospheric radiometric correction the surface reflectance data is obtained, and ready for extraction of the FVC information.

2.3. Dimidiate pixel model for FVC estimation

Assuming the remote sensing response in a pixel consists of soil and vegetation, the information S as captured by the remote sensor can then be expressed as S_v contributed by the green vegetation and S_s contributed by the soil. Linearly decomposing S into S_v and S_s, the proportion of vegetation area in the pixel (f_c) is the FVC of that pixel, and accordingly the proportion of soil area will be $1-f_c$. Assuming the spectral response received by the all-vegetation "pure" pixel is S_{veg}, the information contributed by vegetation in the mixed pixel is S_v, and the spectral response contributed by vegetation in the mixed pixels can be expressed as the product of S_{veg} and f_c:

$$S_v = f_c \times S_{veg} \tag{1}$$

Similarly, assuming the remotely sensed information received by the "pure" soil pixel is S_{soil}, and the information S_s as contributed by soil in the mixed pixel can be expressed as the product of S_{soil} and $1-f_c$:

$$S_s = (1-f_c) \times S_{\rm soil} \tag{2}$$

Based on Eqs. (1) and (2), the spectral response of a mixed pixel can be derived:

$$S = f_c \times S_{veg} + (1-f_c) \times S_{\rm soil} \tag{3}$$

Eq. (3) can be understood as linearly decomposing S into S_{veg} and S_{soil}, whose weights are the proportion of area taken by them respectively in the pixel, that is, f_c and $1-f_c$.

In the case elements other than vegetation and soil are included, such as water body, Eq. (3) should be modified by the multi-component mixed model. In the case of a mixture of only vegetation and soil (dimidiation of a pixel), the FVC can be derived by modifying Eq. (3) as:

$$f_c = \frac{(S - S_{soil})}{(S_{veg} - S_{soil})} \tag{4}$$

where S_{soil} and S_{veg} are the spectral responses from pure soil and pure vegetation pixels, respectively. The model has a fairly sound theoretical basis, and is widely applicable regardless of the geographical constraints. In addition, a major advantage of the dimidiate pixel model is that the impacts from atmosphere, soil background and vegetation type are reduced. S_{soil} contains the soil information including the contribution to remotely sensed data by elements like the type, color, brightness and moisture of soil, while S_{veg} contains the vegetation information including the contribution to the remotely sensed data by elements like type and structure of vegetation. In fact the dimidiate pixel model is a linear stretch based on the two regulatory factors of S_{soil} and S_{veg}, whereby the impacts on remotely sensed data by atmosphere, soil background and vegetation type are reduced to the minimum. Therefore, FVC can be estimated by Eq. (4).

In the dimidiate pixel model, remotely sensed spectral response is well related linearly to the FVC. For instance, the most widely applied remote sensing response is NDVI, which, being the best indicator for plant growth and density of vegetation spatial distribution, is linearly correlated to vegetation distribution density. The value of NDVI, which comprehensively reflects the vegetation type, canopy pattern and growth status in per unit pixel, is determined by elements like the FVC (horizontal density) and LAI (vertical density), and is notably correlated to the FVC. Inserting the NDVI into Eq. (4), we can have the following approximation:

$$f_c = \frac{\mathrm{NDVI} - \mathrm{NDVI}_{soil}}{\mathrm{NDVI}_{veg} - \mathrm{NDVI}_{soil}} \times 100 \tag{5}$$

In Eq. (5), the NDVI for "pure" vegetation pixel and NDVI for "pure" bare soil need to be determined for retrieving the FVC information from remotely sensed data.

2.4. Selection of the narrow band vegetation index

When retrieving the vegetation coverage using the dimidiate pixel model in Eq. (5), the vegetation index calculated from remotely sensed data is required. The hyperspectral imagery has a number of red bands and near infrared bands, resulting in many combinations for calculating narrow band NDVI. Thus, there is a need to determine a more effective combination of bands. In the HJ-1/HSI data there are a total of 22 bands in the near infrared region (760–900 nm) and 15 bands in the red band wavelength region (630–690 nm), and the possible pairs can give a total of 330 NDVI values.

The in situ measured FVC data were used to select an optimal band combination for calculating optimal NDVI in the study. The pairwise comparison of the HJ-1/HSI 330 band combinations for NDVI calculation showed that when the 900 nm near infrared and 682 nm red bands are used to calculate NDVI, the correlation of simple linear regression between NDVI and the in situ measurements

Table 3
Improved model parameters for each land cover type.

Land cover types	HJ-1/HSI	
	$NDVI_{veg}$	$NDVI_{soil}$
Farming lands	0.641	0.071
Grasslands	0.593	0.045
Forest lands	0.576	0.012
Water body	–	–

of FVC is the biggest. Thus, the 900 nm/682 nm band combination is the best for calculating the hyperspectral narrow band NDVI for FVC retrieval in the study area. This band selection method can be easily and quickly implemented in the ENVI/IDL environment.

2.5. Determining the $NDVI_{veg}$ and $NDVI_{soil}$

In the study area, there are "pure" pixels for forests and agricultural areas due to the dense vegetation. In the most areas of this region however, mixed pixels are widespread due to the sparse vegetation and the 100 m resolution of HJ-1/HSI data, and a mixed pixel often containing multiple spectra of elements like soil, vegetation and shadows. Since this study used the dimidiate pixel model for the FVC extraction, the challenge is therefore to identify the correct NDVI values for "pure" vegetation and soil pixels, respectively.

Ideally $NDVI_{soil}$ is not to change with time, and should be around zero for the bare surface. However due to the atmospheric impact and the changes in surface soil moisture, $NDVI_{soil}$ may change with time. In addition, $NDVI_{soil}$ may also change with space depending on conditions like soil moisture, roughness, soil type and color. Therefore it is not practical to think of a fixed and ideal $NDVI_{soil}$ value, as the value will have to change even for the same scene of imagery. For easy adjustment, it is not necessary to know the actual $NDVI_{soil}$ value; instead, it can be extracted based on the image data and the in situ plot measurements.

$NDVI_{veg}$ represents the maximum value of all the vegetation pixels. Depending on the vegetation type, the seasonal change of the canopy, the interference of the foliage background, as well as wet ground, snow and fallen leafs, the determination of the $NDVI_{veg}$ value is similar to that of the $NDVI_{soil}$, as the $NDVI_{veg}$ value will also change with time and space. Therefore, it is not advisable to think of an ideal $NDVI_{veg}$ value either.

To further improve the prediction of the model, the parameters $NDVI_{veg}$ and $NDVI_{soil}$ were determined for the four main land cover types in the study area: farming land, grassland, forest and water body-snow packs. An approach that the FVC results derived by the regressive model is used to resolve the suitable $NDVI_{veg}$ and $NDVI_{soil}$ values for the three main vegetation cover types. For each pixels that in situ measurements are located in, the relationships between the FVC and NDVI can be depicted using the dimidiate pixel model:

$$\begin{bmatrix} fc_1 & 1-fc_1 \\ \vdots & \vdots \\ fc_n & 1-fc_n \end{bmatrix} \begin{bmatrix} NDVI_{veg} \\ NDVI_{soil} \end{bmatrix} = \begin{bmatrix} NDVI_1 \\ \vdots \\ NDVI_n \end{bmatrix} \tag{6}$$

where fc_i is the FVC of the i-th pixel that has in situ measurements. The least-squares method is then used to resolve Eq. (6) and extract the parameters $NDVI_{veg}$ and $NDVI_{soil}$ for the dimidiate pixel models. The parameters for the HJ-1/HSI are listed in Table 3. This method includes the in situ measured FVC that can be seen as prior knowledge into the extraction of the parameters for the dimidiate pixel models. Fig. 3 illustrates the process for determining the parameters for the dimidiate pixel model in this study.

Inserting the dimidiate pixel model parameters derived from spectral mixture de-composition into Eq. (5), FVC of the study area

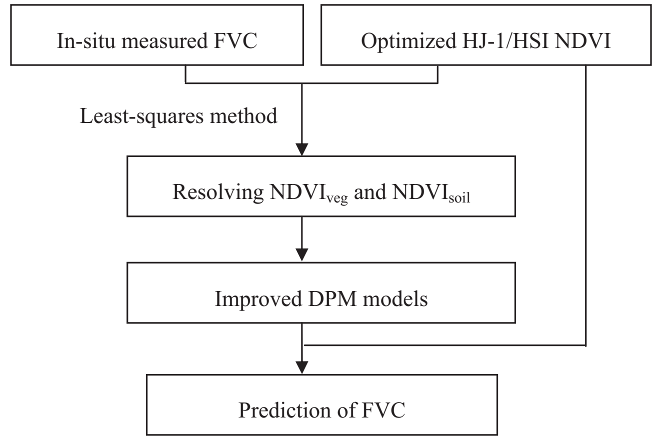

Fig. 3. The flowchart for the extraction of the $NDVI_{veg}$ and $NDVI_{soil}$ parameters.

is retrieved, whose value is between 0 and 100, where 0 represents "pure" bare soil, and 100 represents all or 100% vegetation coverage in the pixel.

3. Results

The above-mentioned dimidiate pixel model was implemented by programming in the ENVI/IDL6.5 environment. The FVC map as of 24 July 2009 of the study area has been obtained using this model (Fig. 4).

As shown in Fig. 4, the northern part of the study area is mainly sand lands with vegetation coverage of less than 5%. Some small patches surrounding the farming land have FVC values between 5% and 20%, but most of them have FVC values of less than 10%. The farming lands are located in the middle part of the area and have FVC values of over 75%, indicating large patches of cotton and grape

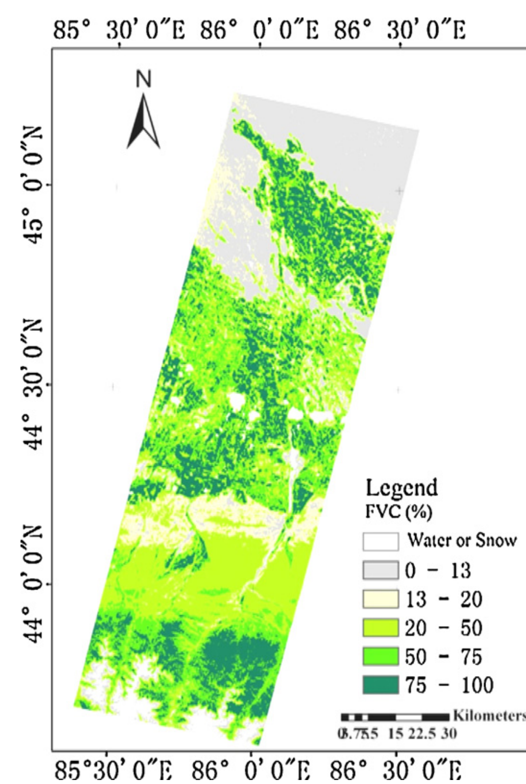

Fig. 4. The FVC map retrieved from the HJ-1/HSI data.

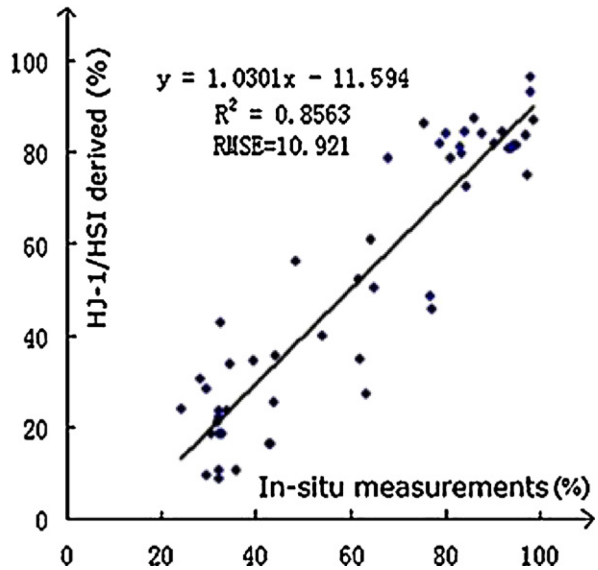

Fig. 5. Fitting analysis between the HJ-1/HSI-derived FVC and in situ measurements.

fields. In the same area, some pixels have FVC values between 50% and 75%, depending on the portion of the densely vegetated cotton and grape fields in a mixed pixel with a 100 m resolution. In the wasteland surrounding the farmland there are some medium vegetation of 20–50% coverage (either farmland or abandoned land), as well as some low coverage sandy land. The steep areas in the piedmont hills of the Tianshan Mountain are sparsely vegetated with FVC values between 5% and 20% due to lack of water content. The type of vegetation is mostly drought tolerant or ephemeral gramineae as well as alhagi pseudalhagi that the cattle and sheep would avoid. With the increase of altitude, some lands are medium vegetated grass and have FVC between 20% and 50%.

At an altitude of 1600–2900 m in the Tianshan Mountains there are distributions of Alpine meadows and Abies forests with the FVC often being above 75% due to much better natural water supply (snow-melting water and larger rainfall) (Fig. 4). In the skirting areas of the forest, high grass lands develop with FVC of over 75%, which are densely vegetated grass land. The averaged FVC values derived from the HJ-1/HSI data for farming land, grassland, forestland and sand land are 64.0%, 30.3%, 68.2%, and 4.9%, respectively.

In general, using the dimidiate pixel model improved by the narrow band spectral indexes of the HJ-1/HSI data, the vegetation distribution of natural vegetation and farmland in the Shihezi area was quantitatively retrieved and well correlated with the landscapes in the area, thus offering an effective means for dynamic monitoring of vegetation.

4. Discussion

4.1. Accuracy assessment

In order to assess the accuracy and viability of the HJ-1/HSI data in vegetation monitoring, this study made a cross-check of ground quadratic data and the FVC results retrieved from the HJ-1/HSI data. 65 in situ measurements in grassland and farming land were used to do the fitting analysis for accuracy assessment. Fig. 5 shows the result of cross-checking the FVC as retrieved from the HJ-1/HSI against the 65 in situ measurements. Obviously the vegetation coverage retrieved from the HJ-1/HSI data fits well with the quadrate results, with a correlation coefficient square of 0.86. The root mean square error (RMSE) of the FVC values retrieved from HJ-1/HSI with reference to the measured values is 10.92%. Although the ground survey also gives errors, generally speaking, the fitting analysis still indicates that the HJ-1/HSI narrow band vegetation index in the decomposition of the mixed pixels can better determine the parameters of the FVC retrieval model, to improve the dimidiate pixel model, so as to better depict the vegetation cover variations in the study area.

4.2. Discussion

Fractional vegetation cover (FVC) information is an important ecological parameter to characterize land surface vegetation condition and ecosystems as well as phonologic sequences in agriculture. As shown in Figs. 4 and 5, the proposed approach can accurately retrieve the FVC information in the study area. However, due to the scale effect between the in situ measurements and the HJ-1/HSI estimate, and some other reasons, the errors are still big in some locations, especially in the low-density grassland, where in situ measurements are larger than the HJ-1/HSI estimated FVC values due to the large heterogeneity in the vegetation patches of the study area.

Apart from the aforementioned scale effect, another important factor to bring errors to the estimate is the impact of soil background on the vegetation signatures. Due to the complex spectral response from the soil background (Huete, 2004), it strongly affects remote sensing observations, and consequently leads to overestimation or underestimation of spectral vegetation indices (Elvidge and Lyon, 1985). Consequently, the FVC retrieved from remotely sensed data has some errors due to the variation of soil background spectra. The narrow band NDVI derived from the HJ-1/HSI data reduced the impact of soil background to some extent due to the fact that the narrow bands were used for the calculation of NDVI. However, the overestimation of NDVI in the northwestern part in Fig. 4 was still observed in this study, but less than the NDVI calculated from broad bands such as Landsat TM because the color of soil or sand in this area is dark.

The other weakness in the proposed approach is the dimidiate pixel model itself in which the subpixel components are decomposed into only two parts: vegetation and non-vegetation. As a matter of fact, the aforementioned soil signatures are quite different due to the organic and mineral components of soil and color. Thus, the spectral signatures of soil in the study area may be used for aiding multiple decomposition of a pixel. Fortunately, the soil color in the arid areas is relatively similar than humid areas due to the various soil water content. As a result the proposed approach reduced the impacts of the soil background and achieved quite accurate estimation of fractional vegetation cover in the Shihezi area.

5. Conclusion

This paper presents an approach to giving better estimation of the parameters for the dimidiate pixel model, to achieve better retrieval of the FVC information in the arid and semi-arid area, and demonstrated the usefulness of the hyperspectral data acquired by Chinese HJ-1/HSI small satellite in the monitoring of vegetation dynamics. We also examined the advantages and disadvantages of the dimidiate pixel model for FVC retrieval in the Shihezi area.

The preprocessing of the HJ-1/HSI data was first discussed, in particular the atmospheric radiation correction method on the basis of the MORDTRAN4 atmospheric transmission model and the determination of the parameters. Secondly, a strategy for using the in situ measured FVC data in selecting the suitable hyperspectral narrow bands for vegetation index calculation was proposed, so as to determine the parameters for the dimidiate pixel model and assess the accuracy of the FVC retrieval. On such basis, the vegetation condition of the second half of July 2009 in Xinjiang's Shihezi area was retrieved using the proposed model established in this study. The retrieved FVC from the HJ-1/HSI data is verified with the in situ measurements, and the correlation coefficient square is 0.86 and the RMSE is 10.9%. The result showed that the FVC information can be accurately estimated by using the HJ-1/HSI data, indicating that the HJ-1/HSI data can satisfy the needs of dynamic and quantitative monitoring of vegetation coverage changes in a medium range.

Further research will mainly focus on the multi-component decomposition of mixed pixels of remotely sensed images, and introducing the pattern recognition methods like matched filters into the establishment of the FVC retrieval models, to remove the complexity of the soil background. We have created a multiple end-member spectral mixture analysis (MESMA) approach to improve the retrieval of FVC information, and will report it in following publication.

Acknowledgements

This study was supported by the Chinese Ministry of Science and Technology through a research grant (No. 2012BAH27B03). The authors would like to thank the China Center for Resources Satellite Data and Application, for providing the HJ-1/HSI data sets. The anonymous reviewers are also acknowledged for their kind and passionate yet detailed comments and suggestions that have helped improve the quality of this manuscript.

References

Anatoly, A.G., Kaufman, Y.J., Stark, R., Rundquis, D., 2002. Novel algorithms for remote estimation of vegetation fraction. Remote Sensing of Environment 80 (l), 76–87.
Asrar, G.F., Myneni, R.B., Choudhury, B.J., 1992. Spatial heterogeneity in vegetation canopies and remote sensing of absorbed photosynthetically active radiation: a modeling study. Remote Sensing of Environment 41, 85–103.
Bannari, A., Mori, D., Bonn, E., 1995. A review of vegetation indices. Remote Sensing Reviews 1995 (13), 95–120.
Boles, S.H., Xiao, X., Liu, J., Zhang, Q., Munkhtuya, S., Chen, S., Ojima, D., 2004. Land covers characterization of Temperate East Asia using multi-temporal VEGETATION sensor data. Remote Sensing of Environment 90, 477–489.
Bonham, C.D., 1989. Measurements for Terrestrial Vegetation. Wiley, New York, p. 352.
Brazel, A.J., Nickling, W.G., 1987. Dust storms and their relation to moisture in the Sonoran-Mojave desert region of the south-western United States. Journal of Environmental Management 24, 279–291.
Chen, J., 1999. Spatial scaling of a remotely sensed surface parameter by contexture. Remote Sensing of Environment 69, 30–42.
Choudhury, B.J., 1987. Relationships between vegetation indices, radiation absorption and net photosynthesis evaluated by a sensitivity analysis. Remote Sensing of Environment 22 (2), 209–233.
Dunean, J., Stow, D., Franklin, J., Hope, A., 1993. Assessing the relationship between spectral vegetation indices and shrub cover in the Jornada Basin, New Mexico. International Journal of Remote Sensing 14 (18), 3395–3416.
Dymond, J.R., Stephens, P.R., Newsome, P.F., 1992. Percent vegetation covers of a degrading rangeland from SPOT. International Journal of Remote Sensing 13 (11), 1999–2007.
Elvidge, C.D., Lyon, R.J.P., 1985. Influence of rock-oil spectral variation on the assessment of green biomass. Remote Sensing of Environment 17 (3), 265–279.
Elvidge, C.D., Chen, Z., 1995. Comparison of broad-band and narrow-band red and near-infrared vegetation indices. Remote Sensing of Environment 54 (l), 38–48.
Godínez-Alvarez, H., Herrick, J.E., Mattocks, M., Toledo, D., van Zee, J., 2009. Comparison of three vegetation monitoring methods: their relative utility for ecological assessment and monitoring. Ecological Indicators 9 (5), 1001–1008.
Graetz, R.D., Pech, R.R., Davis, A.W., 1988. The assessment and monitoring of sparsely vegetated rangelands using calibrated Landsat data. International Journal of Remote Sensing 9 (7), 1201–1222.
Gutman, G., Lgnatov, A., 1998. The derivation of the green vegetation fraction from NOAA/AVHRR data for use in numerical weather prediction models. International Journal of Remote Sensing 19 (8), 1533–1543.
Huete, A.R., 2004. Remote sensing of soils and soil processes. In: Ustin, S.L. (Ed.), Remote Sensing for Natural Resource Management and Environment Monitoring. Manual of Remote Sensing, vol. 4, 3rd edition. John Wiley & Sons, Inc, Hoboken, NJ, USA, pp. 3–52.
Jiang, Z., Huete, A.R., Chen, J., Chen, Y., Li, J., Yan, G., Zhang, X., 2006. Analysis of NDVI and scaled difference vegetation index retrievals of vegetation fraction. Remote Sensing of Environment 101, 366–378.
Jing, X., Yao, W., Wang, J., Song, X., 2010. A study on the relationship between dynamic change of vegetation Coverage and precipitation in Beijing's mountainous areas during the last 20 years. Mathematical and Computer Modelling, 1–7.
Kutiel, P., Cohen, O., Shoshany, M., Shub, M., 2004. Vegetation establishment on the southern Israeli coastal sand dunes between the years 1965 and 1999. Landscape and Urban Planning 67 (1–4), 141–156.
Leprieur, C., Verstraete, M., Pinty, B., 1994. Evaluation of the performance of various vegetation indices to retrieve vegetation cover from AVHRR data. Remote Sensing Reviews 10, 265–284.
Li, Z., Li, X., Wei, D., Xu, X., Wang, H., 2010. An assessment of correlation on MODIS-NDVI and EVI with natural vegetation coverage in Northern Hebei Province, China. Procedia Environmental Sciences 2, 964–969.
Muller-Dombois, D., Ellenberg, H., 1974. Aims and Methods of Vegetation Ecology. Wiley, New York, p. 80.
Neigh, C.S.R., Tucker, C.J., Townshend, J.R.G., 2008. North American vegetation dynamics observed with multi-resolution satellite data. Remote Sensing of Environment 112 (4), 1749–1772.
North, P.R.J., 2002. Estimation of f_{APAR}, LAI, and vegetation fractional cover from ATSR-2 imagery. Remote Sensing of Environment 80 (l), 114–121.
Price, J.C., 1992. Estimating vegetation amount from visible and near infrared reflectance. Remote Sensing of Environment 41, 29–34.
Purevdor, J.T.S., Tateishi, R., Ishiyama, T., 1998. Relationships between percent vegetation cover and vegetation indices. International Journal of Remote Sensing 19 (18), 3519–3535.
Quamby, N.A., Townshend, J.R.G., Settle, J.J., 1992. Linear mixture modeling applied to AHVRR data for crop area estimation. International Journal of Remote Sensing 13 (3), 415–425.
Senseman, G.M., Bagley, C.F., Tweddale, S.A., 1996. Correlation of rangeland cover measure to satellite-imagery-derived indices. Geocarto International 11, 29–37.
Shoshany, M., Kutiel, P., Lavee, H., 1996. Monitoring temporal vegetation cover changes in Mediterranean and arid ecosystems using a remote sensing technique: case study of the Judean Mountain and the Judean Desert. Journal of Arid Environments 33, 9–21.
Steffen, W., 2003. The IGBP terrestrial transects: Tools for resource management and global change research at the regional scale. In: Ringrose, S., Chanda, R. (Eds.), Towards Sustainable Management in the Kalahari Region: Some Essential Background and Critical Issues. , pp. 1–11.
Sykioti, O., Paronis, D., Stagakis, S., Kyparissis, A., 2011. Band depth analysis of CHRIS/PROBA data for the study of a Mediterranean natural ecosystem: correlations with leaf optical properties and ecophysiological parameters. Remote Sensing of Environment 115 (2011), 752–766.
Tammervik, H., Hogda, J.A., Solheim, I., 2003. Monitoring vegetation changes in Pasvik (Norway) and Pechenga in Kola Peninsula (Russia) using multitemporal Landsat MSS/TM data. Remote Sensing of Environment 85 (3), 370–388.
Verstraete, M.M., LePrieur, C., De Brisis, S., Pinty, B., 1993. GEMI: a new index to estimate the continental fractional vegetation cover. In: Proceedings of the 6th AVHRR Data User's Meeting, Belgirate, Italy, 29 June–2 July, pp. 143–149.
Wang, G., Wente, S., Gertner, G.Z., Anderson, A., 2002. Improvement in mapping vegetation cover factor for the universal soil loss equation by geostatistical methods with Landsat Thematic Mapping images. International Journal of Remote Sensing 23 (18), 3649–3667.
Wen, Z., Lees, B.G., Jiao, F., Lei, W., Shi, H., 2010. Stratified vegetation cover index: a new way to assess vegetation impact on soil erosion. CATENA 83 (1), 87–93.
White, M.A., Asner, R.G., Nemani, P.R., Rivette, J.L., Running, S.W., 2000. Measuring fractional cover and leaf area index in arid ecosystem: digital camera, radiation transmittance, and laser altimetry methods. Remote Sensing of Environment 74 (l), 45–57.
Wittich, K.P., Hansing, O., 1995. Area-averaged vegetative cover fraction estimated form satellite data. International Journal of Biometeorology 38 (3), 209–215.
Wu, J., Peng, D., 2010. A research on extracting information of the arid regions' vegetation coverage using improved model of spectral mixture analysis. Multimedia Technology (ICMT), 1–5.
Zhou, Q., 1996. Ground truthing, how reliable is it? In: Proceedings of Geoinformatics'96 Conference, West Palm Beach, FL, 26–28 April. CPGIS, Berkeley, pp. 69–77.
Zhou, Q., Robson, M., 2001. Automated rangeland vegetation cover and density estimation using ground digital images and a spectral-contextual classifier. International Journal of Remote Sensing 22 (17), 3457–3470.